# research papers

# Temperature dependence of the $A$V$_3$O$_7$ ($A$ = Ca, Sr) structure

**Sebastian Prinz,\* Karine M. Sparta and Georg Roth**

Institut für Kristallographie der RWTH Aachen, Jägerstrasse 17-19, 52066 Aachen, Germany

Correspondence e-mail:
prinz@xtal.rwth-aachen.de

The V$^{4+}$ (spin $\frac{1}{2}$) oxovanadates $A$V$_3$O$_7$ ($A$ = Ca, Sr) were synthesized and studied by means of single-crystal X-ray diffraction. The room-temperature structures of both compounds are orthorhombic and their respective space groups are *Pnma* and *Pmmn*. The previously assumed structure of SrV$_3$O$_7$ has been revised and the temperature dependence of both crystal structures in the temperature ranges 297–100 K and 315–100 K, respectively, is discussed for the first time.

## 1. Introduction

A wide variety of interesting topologies and phenomena have been discovered in low-dimensional spin $\frac{1}{2}$ compounds. The common structural element in all three compounds discussed in the following is that the V$^{4+}$ ion is present with square-pyramidal coordination. The alkaline and alkaline-earth metal intercalated V$_2$O$_5$ compounds are examples of low-dimensional vanadates with interesting physical properties (Ueda, 1998). A gap in the magnetic excitation spectrum (spin-gap) at low temperatures or a spin-Peierls transition have been reported for many of these compounds (Smolinski *et al.*, 1998; Lüdecke *et al.*, 1999; Millet *et al.*, 1998; Korotin *et al.*, 1999, 2000). CaV$_4$O$_9$ is another example which has stimulated a lot of interest. It is the first quasi-two-dimensional compound reported to exhibit a spin gap (Taniguchi *et al.*, 1995). Its structure was described in the 1970s (Bouloux & Galy, 1973*a*), but the isostructural SrV$_4$O$_9$ could only be synthesized much more recently (Oka *et al.*, 2000). The $A$V$_4$O$_9$ ($A$ = Ca, Sr) compounds can be characterized as 1/5 depleted square lattices of V$^{4+}$ and their unusual magnetic properties at low temperatures arise from competing nearest (n.n.) and next-nearest neighbour (n.n.n.) interactions within the V$_4$O$_9$ planes (Ueda *et al.*, 1996; Starykh *et al.*, 1996; Sachdev & Read, 1996).

Analogous to the case of $A$V$_4$O$_9$, the $A$V$_3$O$_7$ ($A$ = Ca, Sr, Cd) compounds can be described as 1/4 depleted square lattices, since every fourth pyramidal site remains empty. The structure of CaV$_3$O$_7$ has first been described in a single-crystal X-ray diffraction study (Bouloux & Galy, 1973*b*). Some 20 years later this structure experienced renewed interest, this time with the focus on the relation between the structural and magnetic properties. It was found that CaV$_3$O$_7$ undergoes antiferromagnetic ordering at $T_N \simeq 22$ K (Liu & Greedan, 1993; Harashina *et al.*, 1996) and SrV$_3$O$_7$ orders antiferromagnetically below 34.3 K, as evidenced by neutron powder diffraction (Takeo *et al.*, 1999). The detailed spin structures of SrV$_3$O$_7$ and CaV$_3$O$_7$ have been determined by neutron powder diffraction (Takeo *et al.*, 1999) and Muon Spin Relaxation studies (Fudamoto *et al.*, 2003). The surprising outcome of these studies is that both compounds show a spin

**Table 1**
Experimental and refinement details of $CaV_3O_7$ at selected temperatures.

Full data can be obtained from the CIF file, which has been deposited.

| | 297 K | 250 K | 200 K | 150 K | 100 K |
|---|---|---|---|---|---|
| Crystal data | | | | | |
| Chemical formula | $CaV_3O_7$ | $CaV_3O_7$ | $CaV_3O_7$ | $CaV_3O_7$ | $CaV_3O_7$ |
| $M_r$ | 304.9 | 304.9 | 304.9 | 304.9 | 304.9 |
| Cell setting, space group | Orthorhombic, $Pnma$ | Orthorhombic, $Pnma$ | Orthorhombic, $Pnma$ | Orthorhombic, $Pnma$ | Orthorhombic, $Pnma$ |
| $T$ (K) | 297 (1) | 250 (1) | 200 (1) | 150 (1) | 100 (1) |
| $a, b, c$ (Å) | 10.446 (3), 10.365 (2), 5.2889 (15) | 10.436 (3), 10.367 (2), 5.2921 (15) | 10.426 (3), 10.367 (2), 5.2909 (15) | 10.416 (3), 10.370 (2), 5.2893 (15) | 10.409 (3), 10.374 (2), 5.2876 (15) |
| $V$ (Å$^3$) | 572.6 (3) | 572.6 (3) | 571.8 (3) | 571.3 (3) | 571.0 (3) |
| $Z$ | 4 | 4 | 4 | 4 | 4 |
| $D_x$ (Mg m$^{-3}$) | 3.537 | 3.537 | 3.542 | 3.545 | 3.547 |
| Radiation type | Mo $K\alpha$ | Mo $K\alpha$ | Mo $K\alpha$ | Mo $K\alpha$ | Mo $K\alpha$ |
| $\mu$ (mm$^{-1}$) | 5.670 | 5.671 | 5.678 | 5.683 | 5.687 |
| Crystal form, colour | Parallelepiped, brown | Parallelepiped, brown | Parallelepiped, brown | Parallelepiped, brown | Parallelepiped, brown |
| Crystal size (mm) | $0.3 \times 0.2 \times 0.1$ | $0.3 \times 0.2 \times 0.1$ | $0.3 \times 0.2 \times 0.1$ | $0.3 \times 0.2 \times 0.1$ | $0.3 \times 0.2 \times 0.1$ |
| | | | | | |
| Data collection | | | | | |
| Diffractometer | Stoe IPDS 2 | Stoe IPDS 2 | Stoe IPDS 2 | Stoe IPDS 2 | Stoe IPDS 2 |
| Data collection method | Rotation, $\omega$ scans | Rotation, $\omega$ scans | Rotation, $\omega$ scans | Rotation, $\omega$ scans | Rotation, $\omega$ scans |
| Absorption correction | Numerical | Numerical | Numerical | Numerical | Numerical |
| $T_{min}$ | 0.3188 | 0.3173 | 0.3174 | 0.3169 | 0.3169 |
| $T_{max}$ | 0.4708 | 0.4708 | 0.4708 | 0.4703 | 0.4703 |
| No. of measured, independent and observed reflections | 2489, 389, 365 | 2476, 403, 366 | 2460, 401, 363 | 2461, 399, 366 | 2474, 399, 366 |
| Criterion for observed reflections | $I>2\sigma(I)$ | $I>2\sigma(I)$ | $I>2\sigma(I)$ | $I>2\sigma(I)$ | $I>2\sigma(I)$ |
| $R_{int}$ | 0.0298 | 0.0336 | 0.0331 | 0.0329 | 0.0321 |
| $\theta_{max}$ (°) | 22.93 | 22.97 | 22.98 | 22.99 | 22.86 |
| | | | | | |
| Refinement | | | | | |
| Refinement on | $F^2$ | $F^2$ | $F^2$ | $F^2$ | $F^2$ |
| $R[F^2>2\sigma(F^2)]$, $wR(F^2)$, $S$ | 0.0228, 0.0536, 1.277 | 0.0222, 0.0552, 0.941 | 0.0220, 0.0567, 0.934 | 0.0219, 0.0545, 0.929 | 0.0212, 0.0545, 0.945 |
| No. of reflections | 389 | 403 | 401 | 399 | 399 |
| No. of parameters | 38 | 38 | 38 | 38 | 38 |
| Weighting scheme | $w = 1/[\sigma^2(F_o^2) + (0.0331P)^2]$, where $P = (F_o^2 + 2F_c^2)/3$ | $w = 1/[\sigma^2(F_o^2) + (0.0472P)^2]$, where $P = (F_o^2 + 2F_c^2)/3$ | $w = 1/[\sigma^2(F_o^2) + (0.0493P)^2]$, where $P = (F_o^2 + 2F_c^2)/3$ | $w = 1/[\sigma^2(F_o^2) + (0.0477P)^2]$, where $P = (F_o^2 + 2F_c^2)/3$ | $w = 1/[\sigma^2(F_o^2) + (0.0472P)^2]$, where $P = (F_o^2 + 2F_c^2)/3$ |
| $(\Delta/\sigma)_{max}$ | < 0.0001 | < 0.0001 | < 0.0001 | < 0.0001 | < 0.0001 |
| $\Delta\rho_{max}$, $\Delta\rho_{min}$ (e Å$^{-3}$) | 0.36, −0.31 | 0.36, −0.37 | 0.23, −0.29 | 0.27, −0.28 | 0.24, −0.28 |
| Extinction method | $SHELXL$ | $SHELXL$ | $SHELXL$ | $SHELXL$ | $SHELXL$ |
| Extinction coefficient | 0.020 (2) | 0.0175 (16) | 0.021 (2) | 0.0188 (19) | 0.0180 (18) |

stripe ordering (an arrangement of interpenetrating antiferromagnetic zigzag chains), but the spins are oriented out-of-plane in the former and in-plane in the latter case.

Until now only four-circle single-crystal X-ray diffraction data for $Ca_{1-x}Sr_xV_3O_7$ ($x = 0, 0.45$) and $Cd_{1-x}Ca_xV_3O_7$ ($x = 0, 1$) at room temperature, as well as measurements of magnetization and electron paramagnetic resonance have been published (Nishiguchi *et al.*, 2002), but no single-crystal data for the end-member $SrV_3O_7$ were available. The temperature dependence of the two structures have not been reported either. In previous studies $SrV_3O_7$ was assumed to be isostructural with $CaV_3O_7$ or to crystallize in a noncentrosymmetric space group. Since structural details such as V—O—V angles, V—V and V—O distances are crucial for the magnitude of the magnetic exchange interactions of the nearest and next-nearest neighbours, the temperature dependence of the structural parameters is reported in detail in this work.

## 2. Experimental

### 2.1. Crystal growth

CaO and $VO_2$ were mixed in a 1:3 molar ratio and pressed into a pellet following the literature procedure (Bouloux & Galy, 1973b). The pellet was then placed in an $Al_2O_3$ crucible that was heated in a furnace under dynamic vacuum conditions to a temperature of 1100 K. After several days the heating was switched off. From the sinter cake single crystals of $CaV_3O_7$ were isolated. $SrV_3O_7$ single crystals were grown by a flux method. A salt mixture of LiCl, RbCl and $SrCl_2$ was first prepared by drying the components separately at 413 K and mixing them in the molar ratio 2:1:1. A 1:1 mixture of $V_2O_3$–$V_2O_5$ powder was then added to the mixture in the flux:$VO_2$ molar ratio 2.5:1. The mixture was ground in an agate mortar and then placed in an $Al_2O_3$ crucible. The crucible was then placed into a glass test tube, which was kept open and immediately placed in a glass gas-washing bottle that was

**Table 2**
Experimental and refinement details of $SrV_3O_7$ at selected temperatures.

Full data can be obtained from the CIF file, which has been deposited.

| | 298 K | 250 K | 200 K | 150 K | 100 K |
|---|---|---|---|---|---|
| **Crystal data** | | | | | |
| Chemical formula | $SrV_3O_7$ | $SrV_3O_7$ | $SrV_3O_7$ | $SrV_3O_7$ | $SrV_3O_7$ |
| $M_r$ | 352.44 | 352.44 | 352.44 | 352.44 | 352.44 |
| Cell setting, space group | Orthorhombic, $Pmmn$ | Orthorhombic, $Pmmn$ | Orthorhombic, $Pmmn$ | Orthorhombic, $Pmmn$ | Orthorhombic, $Pmmn$ |
| $T$ (K) | 298 (1) | 250 (1) | 200 (1) | 150 (1) | 100 (1) |
| $a, b, c$ (Å) | 5.2979 (8), 10.529 (2), 5.3139 (9) | 5.2959 (8), 10.534 (2), 5.3014 (9) | 5.2934 (8), 10.537 (2), 5.2889 (9) | 5.2909 (8), 10.544 (2), 5.2763 (9) | 5.2918 (12), 10.550 (3), 5.2717 (14) |
| $V$ (Å$^3$) | 296.41 (9) | 295.74 (9) | 294.99 (9) | 294.34 (9) | 294.32 (14) |
| $Z$ | 2 | 2 | 2 | 2 | 2 |
| $D_x$ (Mg m$^{-3}$) | 3.949 | 3.958 | 3.968 | 3.977 | 3.977 |
| Radiation type | Mo $K\alpha$ | Mo $K\alpha$ | Mo $K\alpha$ | Mo $K\alpha$ | Mo $K\alpha$ |
| No. of peaks for cell parameters | 10 159 | 11 262 | 11 571 | 11 695 | 10 067 |
| $\theta$ range (°) | 3.84–32.1 | 3.84–32.09 | 3.85–32.09 | 3.85–32.09 | 3.8–32.3 |
| $\mu$ (mm$^{-1}$) | 13.513 | 13.544 | 13.579 | 13.608 | 13.609 |
| Crystal form, colour | Needle, brown | Needle, brown | Needle, brown | Needle, brown | Needle, brown |
| Crystal size (mm) | $0.15 \times 0.1 \times 0.02$ | $0.15 \times 0.1 \times 0.02$ | $0.15 \times 0.1 \times 0.02$ | $0.15 \times 0.1 \times 0.02$ | $0.15 \times 0.1 \times 0.02$ |
| | | | | | |
| **Data collection** | | | | | |
| Diffractometer | Stoe IPDS 2 | Stoe IPDS 2 | Stoe IPDS 2 | Stoe IPDS 2 | Stoe IPDS 2 |
| Data collection method | Rotation, $\omega$ scans | Rotation, $\omega$ scans | Rotation, $\omega$ scans | Rotation, $\omega$ scans | Rotation, $\omega$ scans |
| Absorption correction | Numerical | Numerical | Numerical | Numerical | Numerical |
| $T_{min}$ | 0.2196 | 0.2166 | 0.2176 | 0.2166 | 0.2071 |
| $T_{max}$ | 0.5688 | 0.5682 | 0.5676 | 0.5671 | 0.5669 |
| No. of measured, independent and observed reflections | 5058, 305, 294 | 5060, 305, 295 | 5054, 305, 294 | 5053, 305, 296 | 5327, 321, 307 |
| Criterion for observed reflections | $I > 2\sigma(I)$ | $I > 2\sigma(I)$ | $I > 2\sigma(I)$ | $I > 2\sigma(I)$ | $I > 2\sigma(I)$ |
| $R_{int}$ | 0.0649 | 0.0672 | 0.0679 | 0.0704 | 0.0731 |
| $\theta_{max}$ (°) | 25.49 | 25.82 | 25.85 | 25.85 | 25.48 |
| | | | | | |
| **Refinement** | | | | | |
| Refinement on | $F^2$ | $F^2$ | $F^2$ | $F^2$ | $F^2$ |
| $R[F^2 > 2\sigma(F^2)]$, $wR(F^2)$, $S$ | 0.0329, 0.0777, 1.381 | 0.0335, 0.0776, 1.243 | 0.0348, 0.0803, 1.227 | 0.0362, 0.0799, 1.325 | 0.0337, 0.0793, 1.242 |
| No. of reflections | 305 | 305 | 305 | 305 | 321 |
| No. of parameters | 24 | 24 | 24 | 24 | 24 |
| Weighting scheme | $w = 1/[\sigma^2(F_o^2) + (0.0431P)^2 + 0.0P]$, where $P = (F_o^2 + 2F_c^2)/3$ | $w = 1/[\sigma^2(F_o^2) + (0.0371P)^2 + 1.0548P]$, where $P = (F_o^2 + 2F_c^2)/3$ | $w = 1/[\sigma^2(F_o^2) + (0.0415P)^2 + 0.9218P]$, where $P = (F_o^2 + 2F_c^2)/3$ | $w = 1/[\sigma^2(F_o^2) + (0.0410P)^2 + 0.4275P]$, where $P = (F_o^2 + 2F_c^2)/3$ | $w = 1/[\sigma^2(F_o^2) + (0.0396P)^2 + 1.0644P]$, where $P = (F_o^2 + 2F_c^2)/3$ |
| $(\Delta/\sigma)_{max}$ | $< 0.0001$ | $< 0.0001$ | $< 0.0001$ | $< 0.0001$ | $< 0.0001$ |
| $\Delta\rho_{max}$, $\Delta\rho_{min}$ (e Å$^{-3}$) | 0.82, −0.92 | 0.69, −0.99 | 0.61, −0.86 | 0.60, −1.24 | 0.68, −1.16 |

flushed with argon gas (Ar 5.0, Air products). The sample was heat treated at 750 K for 31 d in a vertical tube furnace and then slowly cooled down to room temperature. From the crystallized flux material small brown $SrV_3O_7$ single crystals could be isolated.

## 2.2. Single-crystal X-ray diffraction

Temperature-dependent single-crystal X-ray diffraction measurements were performed on a two-circle imaging-plate diffractometer (Stoe IPDS 2, Mo $K\alpha$ radiation, tube settings 50 kV and 25 mA, pyrolytic graphite monochromator). The diffractometer was equipped with a Cryostream cryogenic $N_2$-gas blower. For $CaV_3O_7$ 19 data sets ($\omega$ scans between 0 and 180° for $\varphi = 0$°) were collected in the temperature range 100–297 K at intervals of 12.5 K. For $SrV_3O_7$ 11 data sets ($\omega$ scans between 0 and 180° for $\varphi = 0$, 45 and 90° were collected in the temperature range 100–298 K.

The lattice parameters and the intensities of the reflections were obtained with the program *X-AREA* (Stoe & Cie, 2002). Numerical absorption corrections *via* symmetry equivalents were performed using the programs *X-RED* (Stoe & Cie, 1996b) and *X-SHAPE* (Stoe & Cie, 1996a). The room-temperature structures of $CaV_3O_7$ and $SrV_3O_7$ were redetermined using direct methods with the program *SHELXS*97 (Sheldrick, 1997a). The refinements were performed with the program *SHELXL*97 (Sheldrick, 1997b), as implemented in the program suite *WinGX* 1.64.05 (Farrugia, 1999). Experi-
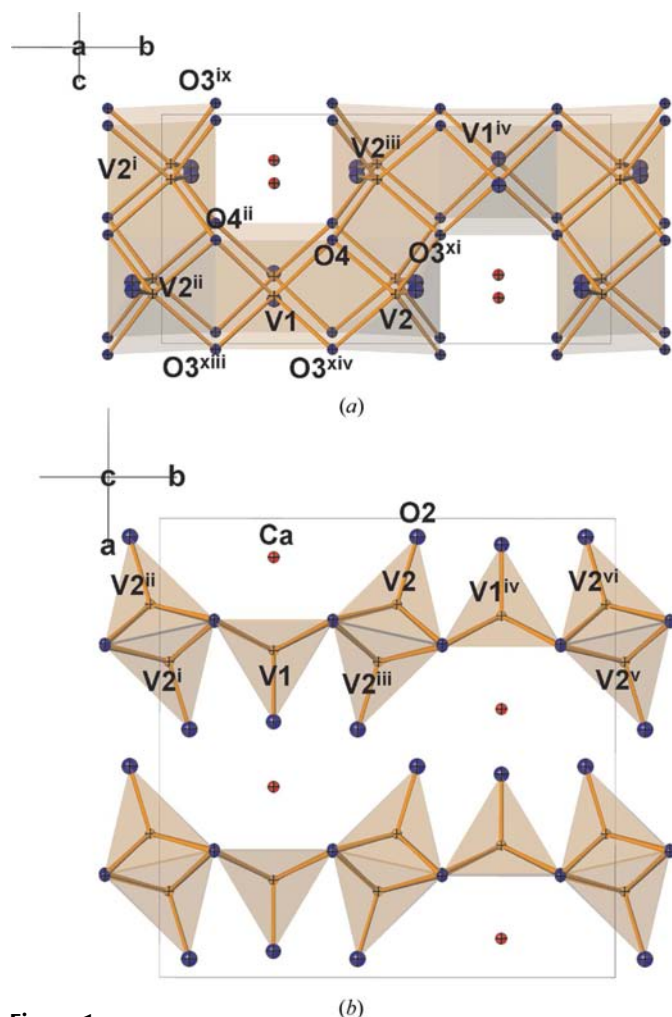
**Figure 1**
Room-temperature structure of CaV$_3$O$_7$ with symmetry codes. (*a*) Projection onto the *bc* plane; (*b*) projection onto the *ab* plane. See Table 3 for the symmetry codes. This and the following molecular graphics were computed with *ATOMS*5.1 (Dowty, 2000).

mental details for five of the 19 structure determinations for the Ca compound, and five of the 11 structure determinations for the Sr compound are summarized in Tables 1 and 2, respectively.[1] Full details for refinements of data measured at the other temperatures are included in the CIF.

## 3. Results

### 3.1. Room-temperature structure of $A$V$_3$O$_7$ ($A$ = Ca, Sr)

CaV$_3$O$_7$ crystallizes in the orthorhombic space group *Pnma* and consists of layers of VO$_5$ pyramids pointing up and down alternately with Ca between the layers (Fig. 1). Note that neighbouring V$_3$O$_7$ layers are not stacked exactly on top of each other, but are offset with respect to each other, which becomes clear in the projection of the unit cell on the *bc* plane

(Fig. 1*a*). The room-temperature cell parameters (Table 1) agree well with the literature data.

The room-temperature structure of SrV$_3$O$_7$, which is very similar to that of CaV$_3$O$_7$, consists of V$_3$O$_7$ layers separated by Sr$^{2+}$ ions (Fig. 2). The layers consist of edge- and corner-sharing VO$_5$ pyramids, the apical O atoms of which point up and down alternately. To our knowledge, the room-temperature structure of SrV$_3$O$_7$ has not been determined by single-crystal X-ray diffraction previously. It has either been assumed to be isostructural to CaV$_3$O$_7$, the structural parameters of which were used as a starting model in the Rietveld refinement from X-ray and neutron powder diffraction data (Liu & Greedan, 1993), or to crystallize in the noncentrosymmetric space group *Pna2$_1$*, as deduced from a positive piezoelectricity test (Bouloux & Galy, 1973*b*). In the present single-crystal X-ray diffraction study of SrV$_3$O$_7$ a unit cell with a lattice parameter perpendicular to the V$_3$O$_7$ layers, which is halved with respect to that in CaV$_3$O$_7$, was found. This is due to the presence of a mirror plane *m* instead of a glide plane as in the case of CaV$_3$O$_7$. We obtained the following lattice parameters: $a$ = 5.2979 (8), $b$ = 10.529 (2) and $c$ = 5.3139 (9) Å. The structure could not be solved in space groups *Pnma* or *Pna2$_1$*, as proposed previously, but in the space groups *Pmmn* and *P2$_1$mn*. The reflection conditions for both space groups are fulfilled and the two solutions show similar refinement results. In a trial the structure was refined in the space group *P2$_1$mn*
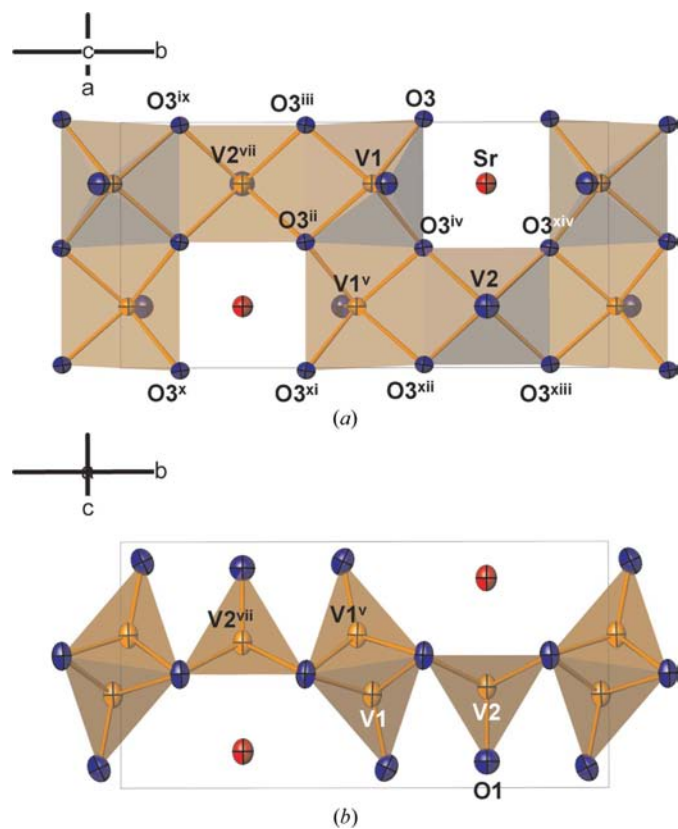


**Figure 2**
Room-temperature structure of SrV$_3$O$_7$ with symmetry codes. (*a*) Projection onto the *ab* plane; (*b*) projection onto the *bc* plane. See Table 4 for the symmetry codes.

**Table 3**
Selected interatomic distances (Å) and angles (°) in $CaV_3O_7$ at 297 K.

| | | | |
|---|---|---|---|
| Ca—O2$^{iii,xviii}$ | 2.346 (4) | V1—V2$^{i,iii}$ | 3.599 (1) |
| Ca—O4$^{ii}$ | 2.393 (3) | V1—O1 | 1.613 (5) |
| Ca—O3$^{ii}$ | 2.432 (3) | V1—O3$^{xiii,xiv}$ | 1.959 (3) |
| Ca—O1$^{xvi}$ | 2.547 (5) | V1—O4$^{ii}$ | 1.970 (3) |
| Ca—O1$^{xvii}$ | 3.540 (5) | V2—O2 | 1.608 (3) |
| V2—V2$^{iii}$ | 2.978 (1) | V2—O4$^{xi}$ | 1.961 (3) |
| V1—V2 | 2.994 (1) | V2—O3$^{xi}$ | 1.966 (3) |
| V1$^{iv}$—V2$^{vi}$ | 3.534 (1) | V2—O3$^{xiv}$ | 1.969 (3) |
| | | | |
| V2—O4—V2$^{iii}$ | 98.9 (1) | V2—O3$^{xi}$—V2$^{iii}$ | 98.5 (1) |
| V1—O4—V2$^{iii}$ | 132.7 (1) | V2—O3$^{xi}$—V1$^{iv}$ | 128.5 (1) |
| V1—O4—V2 | 99.2 (1) | V2—O3$^{xiv}$—V1 | 99.3 (1) |

Symmetry codes: (i) $-x, y-\frac{1}{2}, z-1$; (ii) $x, y+\frac{1}{2}, z$; (iii) $-x, -y+1, -z+1$; (iv) $-x+\frac{1}{2}, -y+1, -z+1$; (v) $-x+\frac{1}{2}, y+\frac{1}{2}, z-\frac{1}{2}$; (vi) $x, -y+\frac{3}{2}, z$; (vii) $-x+\frac{1}{2}, y+\frac{1}{2}, z+\frac{1}{2}$; (viii) $-x+\frac{1}{2}, y-\frac{1}{2}, z-\frac{1}{2}$; (ix) $x, -y+\frac{1}{2}, z$; (x) $-x+\frac{1}{2}, -y+1, z-\frac{1}{2}$; (xi) $-x+\frac{1}{2}, -y+1, z+\frac{1}{2}$; (xii) $-x+\frac{1}{2}, y-\frac{1}{2}, z+\frac{1}{2}$; (xiii) $x, -y+\frac{1}{2}, z+1$; (xiv) $x, y, z+1$.

**Table 4**
Selected interatomic distances (Å) and angles (°) in $SrV_3O_7$ at 298 K.

| | | | |
|---|---|---|---|
| Sr—O2$^{xvii}$ | 2.4843 (7) | V1$^{v}$—V2$^{vii}$ | 3.625 (1) |
| Sr—O3$^{iv,xiv,xvi}$ | 2.5659 (4) | V1—O2$^{i}$ | 1.619 (6) |
| Sr—O1$^{xv}$ | 2.9764 (4) | V1—O3$^{ii,iii}$ | 1.958 (4) |
| Sr—V1$^{xvii}$ | 3.5198 (2) | V1—O3$^{iv}$ | 1.965 (4) |
| Sr—V2$^{xv}$ | 3.5418 (2) | V2—O1$^{i}$ | 1.607 (9) |
| V1—V1$^{v}$ | 2.960 (1) | V2—O3$^{iv,xii,xiii,xiv}$ | 1.976 (4) |
| V1—V2$^{vii}$ | 3.012 (2) | | |
| | | | |
| V1—O3$^{iv}$—V1$^{v}$ | 97.6 (2) | V2—O3$^{iv}$—V1 | 134.2 (3) |
| V2—O3$^{xii}$—V1$^{v}$ | 99.9 (2) | | |

Symmetry codes: (i) $x, y, z+1$; (ii) $x+\frac{1}{2}, -y+1, -z+1$; (iii) $-x, -y+1, -z$; (iv) $-x+\frac{1}{2}, y, z$; (v) $x+\frac{1}{2}, -y+1, -z+1$; (vi) $x+\frac{1}{2}, -y+1, -z$; (vii) $x+\frac{1}{2}, y+\frac{1}{2}, -z+1$; (viii) $x-\frac{1}{2}, y-\frac{1}{2}, -z$; (ix) $-x, y+\frac{1}{2}, -z+1$; (x) $-x+1, y-\frac{1}{2}, -z+1$; (xi) $-x+1, -y+1, -z+1$; (xii) $x+1, y, z$; (xiii) $x+1, y+\frac{1}{4}, z$; (xiv) $-x+\frac{1}{2}, y+\frac{1}{4}, z$; (xv) $x-1, y, z$; (xvi) $x, y+\frac{1}{4}, z$; (xvii) $x, -y+\frac{3}{2}, z$.

as a merohedral twin, but the resulting anisotropic displacement parameters of the O atoms had unreasonably small values, so this space group was rejected. The solution in *Pmmn* was found to be more convincing since the anisotropic displacement ellipsoids of the O atoms were more reasonable, although fewer parameters were used in the refinement.

As mentioned above, VO$_5$ pyramids are the basic structural building units. In $SrV_3O_7$ there are two distinct vanadium positions, V1 and V2. V1O$_5$ pyramids, alternately pointing up and down, form infinite edge-sharing linkages parallel to *a* with V1 showing a site symmetry of *m*... V2O$_5$ pyramids (site symmetry of *mm*2) link up these chains by edge-sharing parallel to *b*. The V sites have a higher site symmetry in $SrV_3O_7$ than the corresponding V sites in $CaV_3O_7$. Consequently, four equivalent V2—O3 basal distances and one short apical vanadyl bond are observed. There are two non-equivalent basal V1—O3 distances which are slightly shorter



**Figure 3**
Clinographic view of the SrO$_8$ distorted tetragonal antiprism with symmetry codes. See Table 4 for the symmetry codes.

than the V2—O3 basal distances. The vanadyl bond found for V1 is slightly longer than that of V2. Selected interatomic distances and angles in $CaV_3O_7$ and $SrV_3O_7$, referred to in the following, are summarized in Tables 3 and 4. Three direct V—V interactions corresponding to the three different V—V distances in $SrV_3O_7$ can be distinguished. The shortest or nearest neighbour (n.n.) V—V distance is that between adjacent V1O$_5$ pyramid centers in the infinite chains of VO$_5$ pyramids, parallel to *a*. The second shortest V—V distance is that between nonequivalent adjacent VO$_5$ pyramids, *i.e.* parallel to *b*. The n.n. and second shortest V—V distances are of similar length. The third shortest V—V distance, and by far the longest, is that between nonequivalent like-oriented VO$_5$ pyramids sharing corners. In $CaV_3O_7$ the situation is somewhat more complicated because four rather than three relevant V—V distances are distinguishable.

$Sr^{2+}$ ions (site symmetry of *mm*2) are located between the layers and coordinated by eight O atoms forming a distorted tetragonal antiprism (Fig. 3). The Sr—O distances can be grouped into three distance ranges: There are two rather long Sr—O1 distances of 2.975 (4) Å, two short Sr—O2 distances of 2.483 (6) Å and four equivalent intermediate Sr—O3 distances of 2.565 (4) Å. As opposed to four different O atoms in $CaV_3O_7$ there are only three nonequivalent O atoms present in the Sr compound. O1 and O2 occupy special positions of site symmetry *mm*2 and *m*.., while O3 is located on a general position. The latter plays a major role in exchange interactions since antiferromagnetism in insulators necessarily involves V—O—V superexchange interactions (Liu & Greedan, 1993). Bouloux & Galy (1973*b*) introduced the tilt angle $\alpha$ between the basal planes of the V1O$_5$ and V2O$_5$ pyramids as a means of characterizing the degree of buckling of the $V_3O_7$ layers. In the following the tilt angle will be named $\delta$, however, in order to avoid confusion with the linear expansion coefficients $\alpha_{ij}$. When comparing the room-temperature structures of $CaV_3O_7$ and $SrV_3O_7$ one can notice a difference in the tilt angles [12.89 (9) and 9.3 (2)°], which is a consequence of the different sizes of the two alkaline-earth cations. Bouloux & Galy (1973*b*) proposed that the larger size of the $Sr^{2+}$ cation leads to a less pronounced buckling of the $V_3O_7$ layers compared with that in the Ca compound, which is
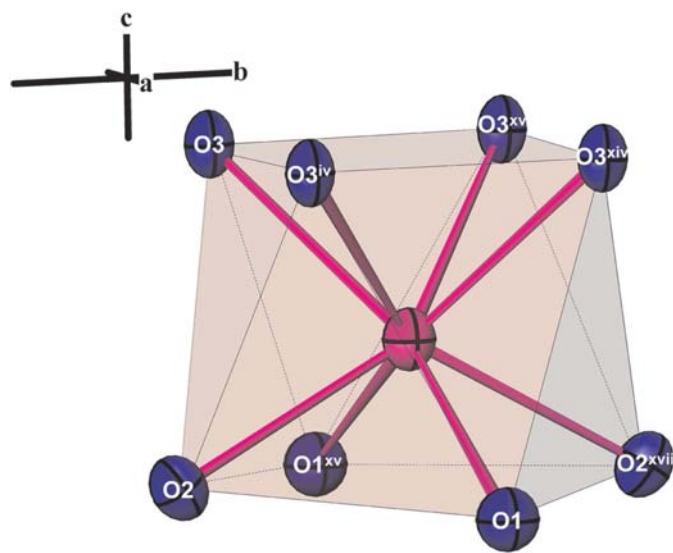
consistent with the smaller $b$ lattice parameter observed for $CaV_3O_7$.

### 3.2. Temperature dependence of the $AV_3O_7$ (A = Ca, Sr) structure

There is no indication of a structural phase transition in the temperature range from room temperature down to 100 K for either compound. The linear thermal expansion coefficients show the same sign for both compounds. The $\alpha_{11}$ values parallel to $a$ and $\alpha_{33}$ values parallel to $c$ in $SrV_3O_7$ are twice as large as the corresponding $\alpha_{33}$ and $\alpha_{11}$ values in $CaV_3O_7$. In
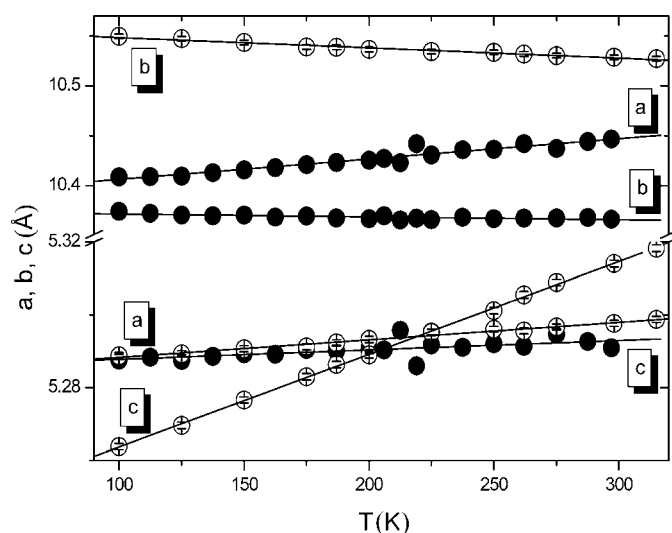


**Figure 4**
Temperature dependence of the cell parameters of $CaV_3O_7$ and $SrV_3O_7$, obtained from single-crystal X-ray diffraction experiments. The least-squares fit lines for $a$, $b$ and $c$ are included in the figure. Note: In this and the following figures filled circles are used to denote $CaV_3O_7$ and empty circles to indicate $SrV_3O_7$. If standard uncertainties are not drawn in any of the figures they are below the symbol size.
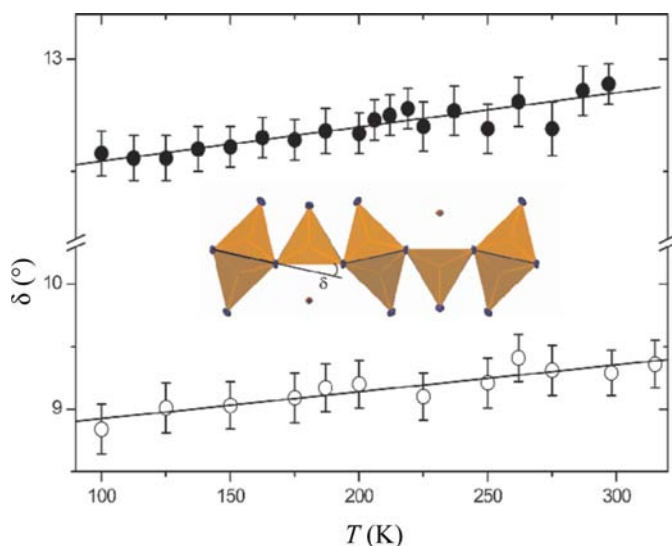
the case of $\alpha_{22}$ they are even three times as large (Table 4). It should be noted that the in-plane lattice parameters $b$ and $c$ ($b$ and $a$) for $CaV_3O_7$ ($SrV_3O_7$) show trends which are opposite each other: While a negative thermal expansion is observed parallel to $b$, *i.e.* perpendicular to the direction of buckling of the $V_3O_7$ layers, positive thermal expansion takes place in the direction at right angles to it (Fig. 4). The negative linear thermal expansion $\alpha_{22}$ parallel to $b$ observed for both compounds corresponds to an increasing corrugation of the layers with increasing temperature, which is expressed by a linear increase of the tilt angle $\delta$ (Fig. 5). The linear-fit curve of the temperature dependence of $\delta$ shows slopes of $1.2\,(2) \times 10^{-4}\,\mathrm{K}^{-1}$ and $2.4\,(3) \times 10^{-4}\,\mathrm{K}^{-1}$ for $CaV_3O_7$ and $SrV_3O_7$. The negative thermal expansion parallel to $b$ results from a competition between thermal expansion and an increasing corrugation of the layers. There are only minimal changes of less than 0.01 Å in the V—O bond lengths of the $VO_5$ pyramids in both $CaV_3O_7$ and $SrV_3O_7$ over the investigated temperature range. The $VO_5$ pyramids can thus be regarded as rigid units. In $CaV_3O_7$ the $VO_5$ pyramids have the freedom to rotate around an axis parallel to $c$ running through the O3 and O4 atoms; in $SrV_3O_7$ the $VO_5$ pyramids similarly rotate around an axis parallel to $a$ running through the O3–O3 edge. This rotational movement can serve as an explanation for the observed negative thermal expansion parallel to $b$.

Both V2—O—V2 bond angles in $CaV_3O_7$ show a linear increase with increasing temperature, which is consistent with the positive thermal expansion along $c$, *i.e.* in the direction of infinite chains of edge-sharing $VO_5$ pyramids (Fig. 6). A linear increase is also observed in $SrV_3O_7$ for the V1—O3—V1 bond angles, which is consistent with the positive thermal expansion parallel to $a$ (Fig. 7). With increasing temperature similar trends are observed for both $CaV_3O_7$ and $SrV_3O_7$: n.n. V—V distances, *i.e.* the distances between equivalent V atoms in the infinite chains of $VO_5$ pyramids show a linear increase of
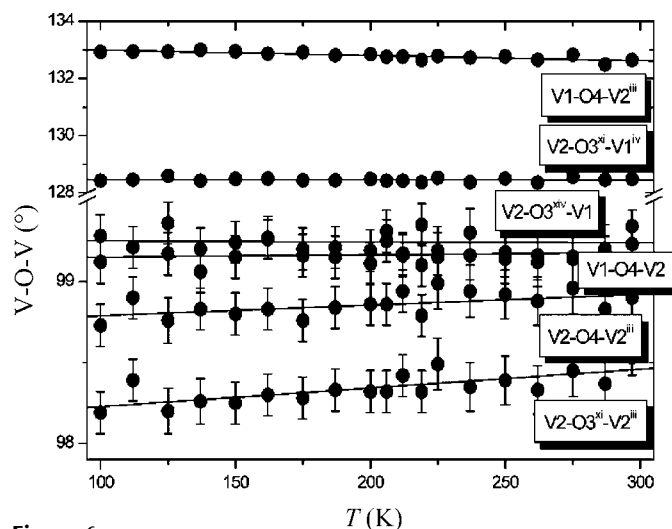


**Figure 5**
Temperature dependence of the tilt angle $\delta$ (shown in the inset) in $CaV_3O_7$ and $SrV_3O_7$. The least-squares fit lines are included in the figure.



**Figure 6**
Temperature dependence of selected V—O—V angles in $CaV_3O_7$. The least-squares fit lines are included in the figure. See Table 3 for the symmetry codes.

0.002 (1) and 0.0071 (6) Å in total over the temperature range from 100 K to room temperature, while the distances between nonequivalent V atoms, *i.e.* the V—V distances between $VO_5$ pyramids pointing upwards and downwards, perpendicular to the infinite chains show a minimal decrease and stay invariant within 1 s.u. (Fig. 8).

## 4. Conclusions

We have synthesized single crystals of $SrV_3O_7$ in a molten salt flux. The structure of $SrV_3O_7$ has been solved by single-crystal X-ray diffraction in the space group *Pmmn* with the lattice parameters *a* = 5.2979 (8), *b* = 10.529 (2), *c* = 5.3139 (9) Å; the
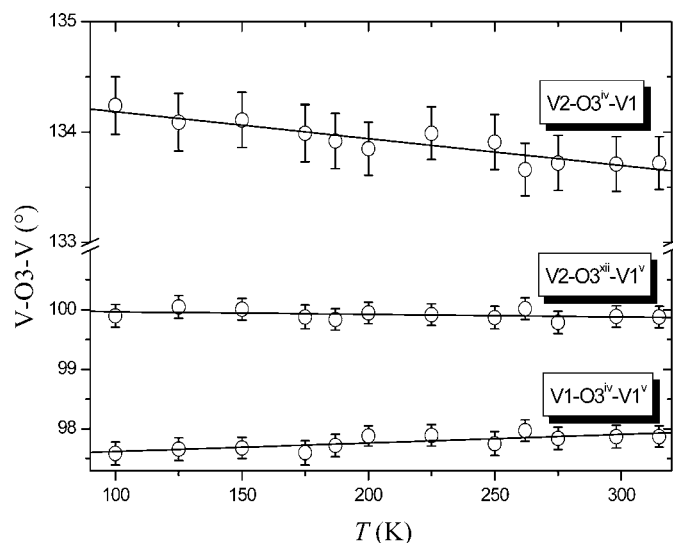
structure of $CaV_3O_7$ has been redetermined in the space group *Pnma* with lattice parameters identical (within 1 s.u.) to those reported in the literature. The temperature dependence of the $AV_3O_7$ (*A* = Sr, Ca) structures was investigated by single-crystal X-ray diffraction in the temperature range from 315 to 100 K and from 297 to 100 K, respectively. The $AV_3O_7$ (*A* = Sr, Ca) structure shows a negative thermal expansion of the lattice parameter perpendicular to the infinite chains of edge-sharing $VO_5$ pyramids which results from a competition between thermal expansion and an increasing corrugation of the $V_3O_7$ layers. The other two lattice parameters show positive thermal expansion. The distinctly different magnetic structures of the two compounds observed by another group (Takeo *et al.*, 1999) need to be readdressed by taking into consideration the fact that the two compounds are not isostructural, as previously assumed.



**Figure 7**
Temperature dependence of the V—O3—V angles in $SrV_3O_7$. The least-squares fit lines are included in the figure. See Table 4 for the symmetry codes.
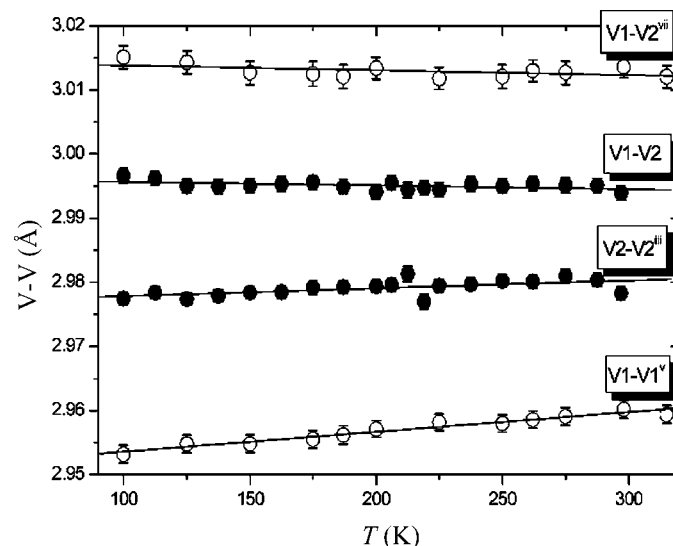


**Figure 8**
Temperature dependence of selected V—V distances in $CaV_3O_7$ and $SrV_3O_7$. The least-squares fit lines are included in the figure. See Tables 3 and 4 for the symmetry codes.

## References

Bouloux, J.-C. & Galy, J. (1973*a*). *Acta Cryst.* B**29**, 1335–1338.
Bouloux, J.-C. & Galy, J. (1973*b*). *Acta Cryst.* B**29**, 269–275.
Dowty, E. (2000). *ATOMS for Windows*, Version 5.1. Shape Software, Kingsport, Tennessee, USA.
Farrugia, L. J. (1999). *J. Appl. Cryst.* **32**, 837–838.
Fudamoto, Y., Gat, I. M., Larkin, M. I., Merrin, J., Nachumi, B., Savici, A. T., Uemura, Y. J., Luke, G. M., Kojima, K. M., Isobe, M., Ueda, Y., Taniguchi, S. & Sato, M. (2003). *Physica B*, **329–333**, 717–718.
Harashina, H., Kodama, K., Shamoto, S., Taniguchi, S., Nishikawa, T., Sato, M., Kakurai, K. & Nishi, M. (1996). *J. Phys. Soc. Jpn*, **65**, 1570–1573.
Korotin, M. A., Anisimov, V. I., Saha-Dasgupta, T. & Dasgupta, I. (2000). *J. Phys. Condens. Matter*, **12**, 113–124.
Korotin, M. A., Elfimov, I. S., Anisimov, V. I., Troyer, M. & Khomskii, D. I. (1999). *Phys. Rev. Lett.* **83**, 1387–1390.
Liu, G. & Greedan, J. E. (1993). *J. Solid State Chem.* **103**, 139–151.
Lüdecke, J., Jobst, A., van Smaalen, S., Morré, E., Geibel, C. & Krane, H.-G. (1999). *Phys. Rev. Lett.* **82**, 3633–3636.
Millet, P., Satto, C., Bonvoisin, J., Normand, B., Penc, K., Albrecht, M. & Mila, F. (1998). *Phys. Rev. B*, **57**, 5005–5008.
Nishiguchi, N., Onoda, M. & Kubo, K. (2002). *J. Phys. Condens. Matter*, **14**, 5731–5746.
Oka, Y., Yao, T., Yamamoto, N., Ueda, M. & Maegawa, S. (2000). *J. Solid State Chem.* **149**, 414–418.
Sachdev, S. & Read, N. (1996). *Phys. Rev. Lett.* **77**, 4800–4803.
Sheldrick, G. M. (1997*a*). *SHELXS*97. University of Göttingen, Germany.
Sheldrick, G. M. (1997*b*). *SHELXL*97. University of Göttingen, Germany.
Smolinski, H., Gros, C., Weber, W., Peuchert, U., Roth, G., Weiden, M. & Geibel, C. (1998). *Phys. Rev. Lett.* **80**, 5164–5167.
Starykh, O. A., Zhitomirsky, M. E., Khomskii, D. I., Singh, R. R. P. & Ueda, K. (1996). *Phys. Rev. Lett.* **77**, 2558–2561.
Stoe & Cie (1996*a*). *X-SHAPE*. Stoe & Cie GmbH, Germany.
Stoe & Cie (1996*b*). *X-RED*. Stoe & Cie GmbH, Germany.
Stoe & Cie (2002). *X-AREA*. Stoe and Cie GmbH, Germany.
Takeo, S., Yosihama, T., Nakajima, K., Isobe, M., Ueda, Y., Kodama, K., Harashina, H., Sato, M., Ohoyama, K., Miki, H. & Kakurai, K. (1999). *J. Phys. Chem. Solids*, **60**, 1153–1155.
Taniguchi, S., Nishikawa, T., Yasui, Y., Kobayashi, Y., Sato, M., Nishioka, T., Kontani, M. & Sano, K. (1995). *J. Phys. Soc. Jpn*, **64**, 2758–2761.
Ueda, Y. (1998). *Chem. Mater.* **10**, 2653–2664.
Ueda, K., Kontani, H., Sigrist, M. & Lee, P. A. (1996). *Phys. Rev. Lett.* **76**, 1932–1935.